

THEORETICAL AND EXPERIMENTAL ANALYSIS OF DISCHARGE SILOS DESIGNS FOR PARTICULATE MATERIALS

H. Mesquita[1], hugo.mesquita@solveengenharia.com.br
M. O. Silva[1], marcelo.silva@solveengenharia.com.br
R.O. Lourenço[1], rol1310@yahoo.com.br
E. F. LINS[2], erb@ufpa.br
A.L.A. Mesquita[2], andream@ufpa.br

[1]Solve Sistemas Industriais Agro-Industriais, Engenharia e Representações Ltda.
[2]School of Mechanical Engineering, Federal University of Pará

Abstract. *In the mining and related industries there are some systems of particulate materials that require appropriate storage and discharge.. During the discharge of such materials, the flow can be interrupted due to the formation of clots in the silos and segregations of the material due the size and other proprieties. Some of these problems can be minimized or eliminated in the appropriate design of the silos. In this paper the theory of Jenike was applied in the development of silos of different geometries and for two types of materials: alumina and kaolin. For these materials, calculations were made as to the maximum angle that should be formed between the conical wall and the vertical reference in the discharge zone of the silo and the minimum diameter so that the flow of the material during the discharge is not interrupted. The influence of the surface of the silo was still analyzed on the flow type. A theoretical model is also analyzed to predict the flow rate of particles and experiments were conducted to develop experimental procedures for proof of the results that were obtained.*

***Keywords**: Jenike cell, Silos, storage, particulate materials.*

1. INTRODUCTION

The rheological behavior of the materials in particle form is complex and cannot be treated as liquids, suspensions or solids. This frequently brings about some handling problems: segregations, flow interruptions during discharge of the materials from the silos and uncontrolled discharge of solids, which can affect the production process negatively. This problem can be minimized with improved design. The discharge of the powder material in can produce in two ways: funnel or mass flow. The existence of a flow type or another will depend on the nature of the bulk material as well as the hopper geometry. As a consequence and in order to design a silo with a certain flow type, the characteristics of both the material and the silo must be considered jointly. Especially, the discharge of powders and granular solids from silos, hoppers, transport containers etc. may result in severe problems, e.g. due to flow obstructions, segregation, shocks and vibrations, or unsteady flow. In order to avoid such complications, solutions have to be found considering the flow properties of the bulk material (Drescher *et al.*, 1995, Drescher and Waters, 1995).

In spite of the frequent bridge occurrences in materials in the silo discharge, the amount of detailed information about the parameters of the material flow, silo geometries, and the feeding discharge condition is very limited (). This lack of detailed information demands a complete verification and critical evaluation of the several existing bridge theories. As the predictions differ, and the experimental results are contradictory there still exist doubts on which theory gives the best results. Great emphasis is given to the comparison of the theoretical prediction of the critical discharge diameter with the results obtained from the tests in silos. In this paper, a numeric code is presented that allows for calculating the output diameter for several materials and silos types. Also is presented a routine that allows for calculating the outflow, given the output size (Enstad, 1975, Arnold and McLean, 1976).

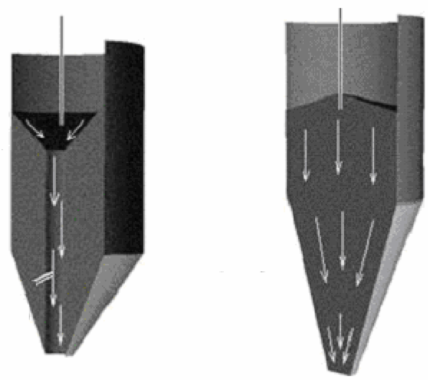

Figure 1 - Discharge patterns from the silos: (right) mass flow; (left) funnel flow.

2. CALCULATION OF THE MINIMUM SILO DIAMETER

2.1. Theoretical expressions for the critical discharge diameter

The most widely used test for determining the properties of bulk solids flow is the direct shear test with the Jenike cell. The simplicity of this test is frequently offset by a limited number of tests or dispersion in the data due to variation in the properties of the material and due to differences in sample preparation. Approaches and averages are then introduced in the process of determination in the way of *IYL* and of *EYL* in the diagram of Mohr and of the flow function ff that relates to ***fc***.

Irrespectively of the method applied, the involved approaches might or might not take the bridge into consideration. Frequently, the objective of the test is to better understand the flow properties of the material or to improve test methodology. All that may lead to some inconsistencies between the considered approach and the theory of the bridge problem formation. In the approach for the structural mechanics, the consideration of a field of radial tensions plays a fundamental role. Without that consideration, the concept of flow function will be no longer valid. This, in turn, requires that the condition of effective yield should have the form given by the equation (1), that is, the covering of the stress consolidation circles of the diagram of Mohr (SC) (Gu *et al.*, 1992a).

$$\sigma_t = \sigma_n \tan\delta \tag{1}$$

$$\sigma_s = \sigma_n \tan\phi + c \tag{2}$$

The approaches involved for the plan of ***IYL*** for the construction of the stress consolidation circles ***(SC)*** and of uniaxial compression (UC) they affect her they form resultant of FF, for the condition that every IYL and EYL are tangent to the same circle ***SC***.

The simple form of IYLs, still appropriate for some materials, and a group of straight lines given by the equation (2) that can be either mutually parallel or competitive. Thus, equations (1) and (2) take the following relationship among ***fc*** and

$$f_c = \frac{2(\mathrm{sen}\,\delta - \mathrm{sen}\,\phi)}{(1+\mathrm{sen}\,\delta)(1-\mathrm{sen}\,\phi)}\sigma_1 \tag{3}$$

If it is the same for all the ***IYLs***, equation (14) is a constant. It implies that ***FF*** is linear and represented by a straight line. The reason for that is the similarity of parallel ***IYLs***, The critical diameter discharge, based on the mechanics of the continuous is certain of the condition that the compressive uniaxial tension of the material ***fc*** the main tension is equal to the main tension 1a acting in the arch. This main tension *1a* is found to add graphically to the flow function FF and the factor of flow ***ff*** to find the intersection point among them or analytically solving the equations that define ***FF*** and ff. for FF a curve is taken passing through the origin of the graph and described by the widespread equation of Warren-Spring.

$$\left(\frac{f_c + E}{E}\right)^q = \frac{\sigma_1}{F} + 1 \tag{4}$$

where F and q are constant material, 1a can be found from

$$\left(\frac{\sigma_{1a}+E}{E}\right)^{q}-\frac{\sigma_{1a}\,ff}{F}-1=0 \qquad (5)$$

where ff is the flow factor. If a non lineal FF is approximate for a linear equation as $f_c = K\,\sigma_1 + L$, then

$$\sigma_{1a}=\frac{L}{1-K\,ff} \qquad (6)$$

Once the tension *1a* is certain, the output size D is found by

$$D=\frac{2\,\sigma_{1a}\,\mathrm{sen}\,\theta_w}{\gamma\,g(\theta_w,\varphi_w)} \qquad (7)$$

where γ the apparent unitary weight, w, is the angle of friction material/wall, and the function *g()* depends on the form that the arch is assumed by the theory. In the theory of Jenike, ff and ***g ()*** are given in graphic form.

In the theory of Enstad based on the mechanics of the continuous, the critical diameter discharge results from the condition that tension doesn't exist supporting the arch underneath. The corresponding expression for D is

$$D=\frac{2\,k\,(\theta_w,\delta^{'},\varphi_w,c^{'})\,\mathrm{sen}\,\theta_w}{\gamma\,h\,(\theta_w,\delta^{'},\varphi_w)} \qquad (8)$$

Where δ' is the angle of friction it executes, c' is the independent consolidation of the cohesion and the functions ***k ()*** and ***h ()***are obtained from this theory. The application of these equations above is limited, in general, for steep and uniform silos, where the mass flow occurs.

The numerical results obtained accomplish the calculation of the functions ff and *g()*. Several models available in the literature use those results to calculate the critical diameter of the silo (Drescher *et al.*, 1995). The correlations used are shown to proceed. The description and its origin are shown in) (Gu et al., 1992b). In all of them, m is the type of the silo (m=1 if it is flat and m=2 if it is conical) and $\beta=\frac{1}{2}\left(\varphi_w + arcsen\frac{sen\,\varphi_w}{sen\,\delta}\right)$

Walker

Case 1: $\theta_w \geq 45^0-\varphi_w$

$$ff=\frac{m(1+sen\delta)}{2\tan\theta_w[sen\,\delta\cos 2(\beta+\theta_w)-1](mH+1)}$$

$$g()=\frac{2sen\,\theta_w}{m}$$

Case 2: $\theta_w < 45^0-\varphi_w$

$$ff=\frac{m(1+sen\delta)\,sen\,2(\theta_w+\varphi_w)}{2\tan\theta_w[sen\,\delta\cos 2(\beta+\theta_w)-1](mH+1)}$$

$$g()=\frac{2sen\,\theta_w}{m\,sen\,2(\theta_w+\varphi_w)}$$

then $H=1-\frac{sen\,\delta\,sen\,2\beta(\cot\theta_w+\cot\varphi_w)}{1-sen\,\delta\cos 2(\beta+\theta_w)}$

Mróz and Szymanski

Case 1:

$$ff=\frac{M\,(1+sen\delta)[(2-m)0.72+(m-1)1.30]}{sen\,\theta_w[sen\,\delta\cos 2\beta-1](mN+1)}$$

$$g()=2sen\,\theta_w[(2-m)0.69+(m-1)0.38]$$

Case 2: $\theta_w < (2-m)67^0 + (m-1)60^0 - \varphi_w$

$$ff = \frac{M(1+sen\delta)\,sen^2(\theta_w+\varphi_w)[(2-m)+(m-1)\,sen(\theta_w+\varphi_w)]}{sen\theta_w[sen\delta\cos 2\beta - 1](mN+1)\{(2-m)(\theta_w+\varphi_w)+(m-1)[1-\cos(\theta_w+\varphi_w)]\}}$$

$$g() = \frac{sen\theta_w}{sen^2(\theta_w+\varphi_w)}\left[(2-m)[\theta_w+\varphi_w]+(m-1)\frac{1-\cos(\theta_w+\varphi_w)}{sen(\theta_w+\varphi_w)}\right]$$

then $\begin{cases} M = (2-m)\dfrac{\theta_w}{sen\theta_w} + (m+1)\dfrac{2}{1\_\cos\theta_w} \\ N = 1 - \dfrac{sen\delta\,sen 2\beta(\cot\theta_w + \cot\varphi_w)}{1 - sen\delta\cos 2\beta} \end{cases}$

Arnold and McLean

$$ff = \frac{S(1+sen\delta)}{T(U-1)sen\theta_w}\left(\frac{1.13}{2.16+\theta_w}\right)^{1-m}\left(\frac{2.48}{3.48+\theta_w}\right)^{m-2}$$

$$g() = 2sen\theta_w\left(\frac{1.13}{2.16+\theta_w}\right)^{1-m}\left(\frac{2.48}{3.48+\theta_w}\right)^{m-2}$$

then $\begin{cases} S = [2-2\cos(\beta+\theta_w)]^{m-1}(\beta+\theta_w)^{2-m}\,sen\theta_w + sen\beta\,sen^m(\beta+\theta_w) \\ T = 2(1-sen\delta)\,sen^m(\beta+\theta_w) \\ U = \dfrac{2^{m-1}sen\delta}{1-sen\delta}\left[\dfrac{sen(2\beta+\theta_w)}{sen\theta_w}+1\right] \end{cases}$

Enstad

$$k() = c\acute{}\left(2^{m-1}sen\delta\acute{}\left[1+\frac{sen(\beta+\theta_w)}{sen\theta_w}\right]-1\right)$$

$$h() = \frac{sen\beta\,sen^m(\beta+\theta_w)+[2-2\cos(\beta+\theta_w)]^{m-1}(\beta+\theta_w)^{2-m}\,sen\theta_w}{2\tan\delta\acute{}\,sen^{m+1}(\beta+\theta_w)}$$

2.2. Mass Flow determination

The prediction of mass flow regime in silo is one of the major problems faced in the storage of materials in bulk. This prediction is of underlying importance for the design of the conveying line and output diameter of the silo. Due to the peculiar characteristics of the material in bulk, the study of behavior due to complex flow, once the size of the particle prevents it from being treated continuously and from treating each particle like an independent entity, is still unfeasible in computational terms. In this research work, numerical code was developed and allows for determining the flow in a silo in accordance with the foundations of the continuum mechanics. In order to increase the reliability of this evaluation, the work take into account one of the most important factors during the flow: the gradient of air pressure inside the silo (Gu *et al.*, 1992).

The adopted numerical procedure uses the models available in the literature (Drescher and Waters, 1995). The first is a module that encapsulates all the necessary functions to calculate the distribution of pressure density inside the silo. The second step makes the calculation of the mass flow. Initially, calculations are made to obtain some other geometric parameters of the silo and to simplify variables given by the equation(8). Before proceeding with the density calculations, it is necessary to make a reasonable estimate of K(3) parameter, since it is necessary for calculating the mp. This was made by using the continuity of the density gradient in the interface between areas II and III, like Figure 2.

$$\eta = \frac{h}{h_1};\quad \eta_0 = \frac{h_0}{h_1};\quad \eta_{max} = \frac{h_{max}}{h_1};\quad \eta^* = \frac{h^*}{h_1};\quad \eta_{mp} = \frac{h_{mp}}{h_1};\quad H\acute{} = \frac{H}{h_1} \qquad (8)$$

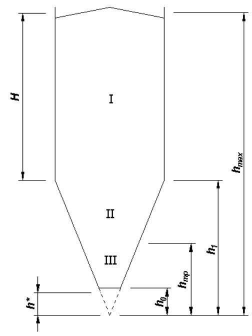

Figure 2 - Regions defined for a mass flow bin.

The equations (9) and (10) are integrated. Newton's method is used to find the value of K3. The pressure and density value results are sent for a text file.
In region III and II:

$$\tilde{P} = \frac{P}{W_o} = \int_{\eta_0}^{\eta} \frac{f_2^{a-1} - (1-K_{dea}) f_2^{a}}{(\eta/\eta_0)^2} d\eta \tag{9}$$

in transition point $\tilde{P}_1 = \frac{P_1}{W_o} = \int_{\eta_0}^{\eta} \frac{f_2^{a-1} - (1-K_{dea}) f_2^{a}}{(\eta/\eta_0)^2} d\eta$

In region I:

$$\tilde{P} - \tilde{P}_1 = \frac{P - P_1}{W_0} = \left(\frac{\eta_0}{\eta_1}\right)^2 \int_{\eta_1}^{\eta} \left[f_1^{a-1} - (1-K_{dea}) f_1^{a} \right] d\eta \tag{10}$$

The pressure in the silo is directly proportional to W_0, and this depends on the mass flow. I just interested in the value of Kdea, the pressure dimensional allows for obtaining that value easily. After this step, we can obtain the value of the mass flow through the equation (11).

$$a_{11} Q_p^2 + b_{11} Q_p - c_{11} = 0 \tag{11}$$

3. EXPERIMENTAL SETUP

3.1. Jenike Cell

Standard Shear Testing Method for Bulk Solids was employed by using the Jenike Shear Cell. This method covers the apparatus and procedures for measuring the cohesive strength of bulk solids during both continuous flow and after storage at rest. In addition, measurements of internal friction, bulk density, and wall friction on various wall surfaces are included. The most common use of this information is in the design of storage bins and hoppers to prevent flow stoppages due to arching and ratholing, including the slope and smoothness of hopper walls to provide mass flow. Parameters for structural design of such equipment may also be derived from this data. The executed experimental procedure is accomplished as described in the norm (*AST*, 1997).

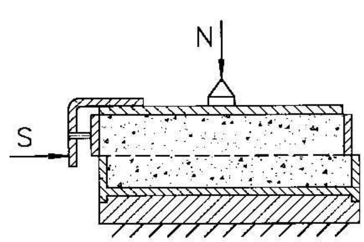

Figure 3 - Material submitted to the shear process (*AST*, 1997).

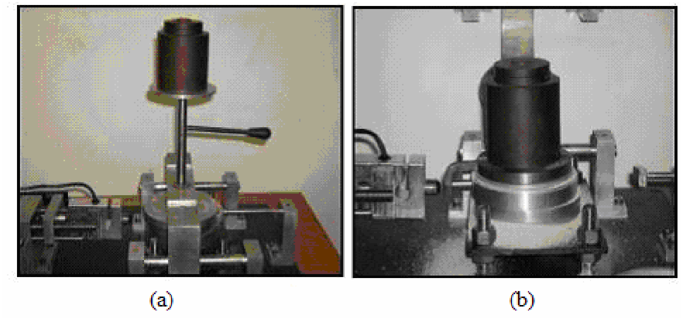

Figure 4 - Jenike Cell built at the laboratory, (a) sample under torsion (b) Shear process.

3.2. Prototype of silos with different discharge diameters

The silo prototype developed at the laboratory has 28 cm in diameter in the circular area and 50cm in height (cylindrical region, according Figure 5). It was built to allow for changing the conical region, for different values of discharge diameters and inclinations, and is in accordance with the need of the tests. It is made from PET transparent material for ease of visualization of the flow.

Figure 5 – Silo prototypes.

4. RESULTS AND DISCUSSION

The results presented for determination of the attrition angle between product and material of the silo wall Øw are due to the behavior analyzed in test in the Jenike cell between the alumina and the Kaolin, and a sample of the PET material used for making the prototype. The obtained results are visualized by the tables 1 and 2, and Figure 6. The values of tensions introduced in the program PPF are those whose angle value Øw came larger; in other words, Øws for the applications for the calculation of the factor flow of the area conical *ff* according to the theory of Enstad, 1975. The following results were then achieved for the alumina attrition test with a sample of the alumina from the silo wall.

Table 1. Alumina values of tensions for the first test for determination of the $Ø_w$.

Normal Stress (Pa)	Shear Stress (Pa)
7057,54	3105,32
5646,03	2399,56
4234,52	1976,11
2823,01	1270,36
1411,51	705,75
597,80	423,45

Table 2. Kaolin tension values for the first test for determination of the $Ø_w$.

Normal Stress (Pa)	Shear Stress (Pa)
7071,534	1909,314
5657,227	1541,594
4242,921	1178,589
2828,614	825,012
1414,307	466,721
707,153	282,861

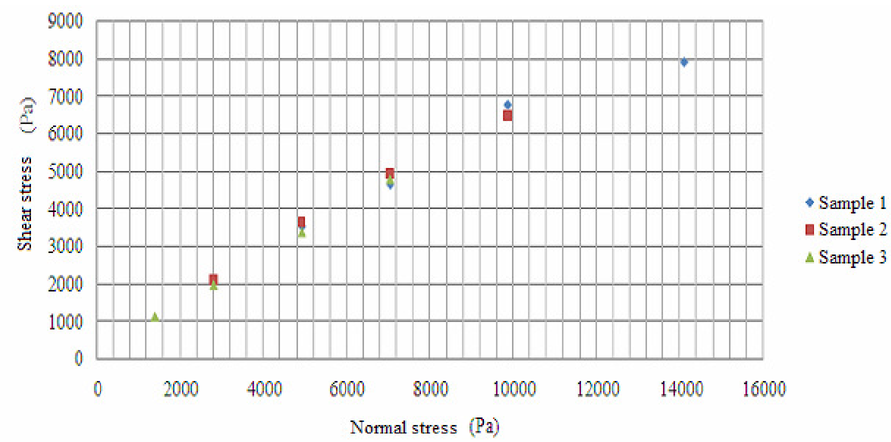

Figure 6 – Fluency curve for Alumina.

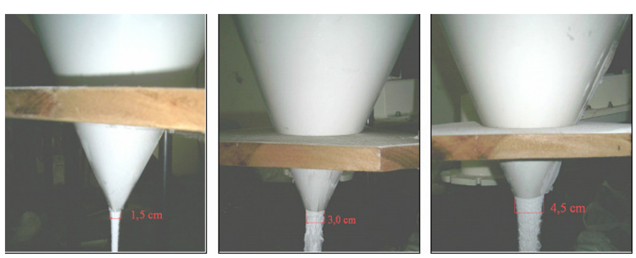

Figure 7 - Different drainage conditions in different discharge diameters for Alumina.

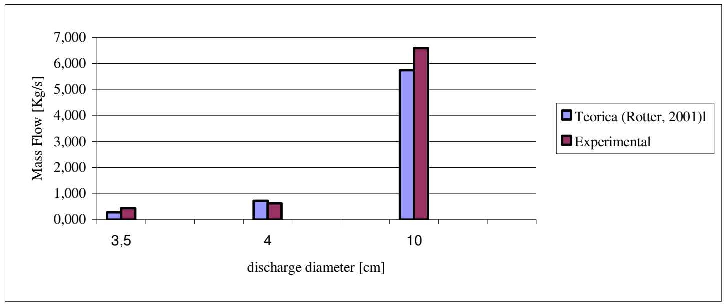

Figure 8 – Mass flow rate for kaolin.

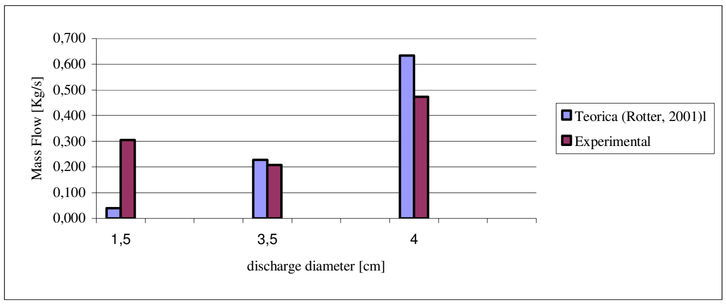

Figure 9 - Mass flow rate for alumina.

This research work could offer a study on the main necessary stages for the characterization of a product aiming at storage in silos, and some peculiarities regarding the classification and characteristics in what are due after the project of a storage silo. It presents results with experimental validation to the theories and a methodology adopted for the characterization of the physical properties of bulk materials

The procedure gives a good way to predict the critical discharge diameter for design purpose and to calculate the mass flow rate from silo with a defined geometry, according figures 7, 8 and 9.

5. ACKNOWLEDGEMENTS

The authors would like to express their gratitude for the financial support from CNPQ (proc. no. 560832/2008-7), without which this paper would be impossible.

6. REFERENCES

Drescher, A.J. Waters, C. A. Rhoades, *Arching in hoppers: I. Arching theories and bulk material flow properties*, Powder Technology, 84, 1995.

Drescher, A.J. Waters, C. A., *Arching in hoppers: II. Arching theories and critical outlet size*, Powder Technology, 84, 1995.

Drescher, , A.J., *On the criteria for mas flow in hoppers*, Powder Technology, 73, 1992.

Enstad , G., *On the theory of arching in mass flow hoppers*, Chemical Engineering Science, vol.30, 1975.

Arnold, P. C. McLean, A. G., *An analytical solution for the stress function at the wall of a converging channel*, Powder Technology, 13, 1976.

Gu, Z. H., Arnold, P. C. McLean, A. G. *Consolidation-related bulk density and permeability models for bulk solids*, Powder Technology, 72, 1992.

Gu, Z. H. , Arnold , P. C., A. G. McLean, *Modeling of air pressure distributions in mass flow bins, Powder Technology*, 72, 1992.

Gu, Z. H., Arnold, P. C., McLean, A. G. *Prediction of the flowrate of bulk solids from mass* flow bin with conical hoppers, Powder Technology, 72, 1992.

American society for testing and materials (AST), *Standard Shear Testing Method for Bulk Solids Using the Jenike Shear Cell*, , Designation: D 6128 – 97.

7. RESPONSIBILITY NOTICE

The author(s) is (are) the only responsible for the printed material included in this paper.